




Article

Electricity Generation at Gas Distribution Stations from Gas Surplus Pressure Energy

Serhii Vanieiev ¹, Jana Mizakova ², Dmytro Smolenko ¹, Dmytro Miroshnychenko ³, Jan Pitel ^{2,*}, Vadym Baha ¹ and Stanislav Melechuk ¹

- ¹ Department of Technical Thermal Physics, Faculty of Technical Systems and Energy Efficient Technologies, Sumy State University, 116, Kharkivska St., 40007 Sumy, Ukraine; s.vaneev@kttf.sumdu.edu.ua (S.V.); d.smolenko@kttf.sumdu.edu.ua (D.S.); v.baga@kttf.sumdu.edu.ua (V.B.); s.melechuk@zaoch.sumdu.edu.ua (S.M.)
- ² Department of Industrial Engineering and Informatics, Faculty of Manufacturing Technologies, Technical University of Kosice, 1, Bayerova St., 08001 Presov, Slovakia; jana.mizakova@tuke.sk
- ³ Department of Manufacturing Engineering, Machines and Tools, Faculty of Technical Systems and Energy Efficient Technologies, Sumy State University, 116, Kharkivska St., 40007 Sumy, Ukraine; 116mirdv@gmail.com
- * Correspondence: jan.pitel@tuke.sk; Tel.: +421-905-241605

Abstract: At gas distribution stations (GDSs), the process of throttling (pressure reduction) of natural gas occurs on gas pressure regulators without generating useful energy. If the gas expansion process is created in a turbine, to the shaft where an electric generator is connected, then electricity can be obtained. At the same time, the recycling of secondary energy resources is provided, which is an important component in the efficient use of natural resources. The obtained electric power can be supplied to the external power grid and/or used for the GDS's own needs. The process of generating electricity at the GDS from gas overpressure energy is an environmentally friendly, energy-saving technology that ensures an uninterrupted, autonomous operation of the GDS in the absence of an external energy supply. The power needs of a GDS with regard to electricity are relatively small (5 ÷ 20 kW). Expansion in throttling devices or turbine flow paths leads to gas cooling with a possible hydrate formation. It is prevented via gas preheating or vortex expansion equipment that keeps the further gas temperature at a necessary level. Turbogenerators can be created on the basis of vortex expansion turbomachines, which have many advantages compared to turbomachines of other types. This article studies how gas pressure (outlet: gas distribution station) and gas preheating (inlet: vortex expansion machine) influence turbogenerator parameters. Nine turbogenerator variants for the power needs of gas distribution stations have been assessed.

Keywords: gas expansion processes; gas heating; power generation; gas distribution station; energy-saving turbine generator; vortex turbine



Citation: Vanieiev, S.; Mizakova, J.; Smolenko, D.; Miroshnychenko, D.; Pitel, J.; Baha, V.; Melechuk, S. Electricity Generation at Gas Distribution Stations from Gas Surplus Pressure Energy. *Processes* **2024**, *12*, 1985. <https://doi.org/10.3390/pr12091985>

Academic Editors: Ferdinando Salata and Virgilio Ciancio

Received: 7 August 2024

Revised: 7 September 2024

Accepted: 9 September 2024

Published: 14 September 2024



Copyright: © 2024 by the authors. Licensee MDPI, Basel, Switzerland. This article is an open access article distributed under the terms and conditions of the Creative Commons Attribution (CC BY) license (<https://creativecommons.org/licenses/by/4.0/>).

1. Introduction

The Ukrainian gas grid is a complex system with a changing load. Its separate elements require modernization. Since resource economy is a must, the system may be complicated to secure a higher level of efficiency. One of the necessary technical decisions is differential pressure with a subsequent useful output instead of energy loss in the case of gas throttling on pressure regulators. Here, turboexpanders may recycle the gas pressure excess, while mechanical work on turbine shafts is converted into electric power [1,2]. This is an efficient technology to generate clean energy. In Ukraine, there are 1450 gas distribution stations (GDSs). The working pressure of gas mains is 5.5 ÷ 7.4 MPa, with a possible fall to 2.5 MPa. Reduced to 0.3, 0.6, or 1.2 MPa, the station gas is gradually transferred to the distribution network, control points, and then to consumers. Simultaneously, the energy of gas pressure excess is lost.

Vortex expansion is efficiently used in turboexpanders and turbogenerators up to 500 kW [1,3]. The same may be realized in cogeneration units (heat and energy supply for industrial and community facilities), turbine starters, control systems, turbocompressors, pumps, etc. For a 100 kW turbogenerator, the annual profit from the generated power (power price USD 0.07) is as follows: $0.07 \times 100 \text{ kW} \times 8000 = 56,000 \text{ USD}$ per year. Installed turbogenerators on gas distribution stations and control points are estimated to provide about 10,500 million UAH per year (for electricity tariff at 2.6 UAH per kWh). You can benefit more if turbogenerators are located in engineering, food, chemical, or community facilities. Additionally, turbogenerators raise power supply reliability, state energy security, and ecological performance. Today, it is urgent to increase the gas distribution efficiency via the construction of autonomous uninterruptible power sources on the station itself. Although the gas distribution station capacity is under 20 kW, their permanent work determines the functionality of the whole station's technological process until the gas is supplied to consumers. These uninterruptible power sources should be based on vortex turbines. Such a machine may constantly operate on the station as a power-saving turbogenerator. Figure 1 shows a gas distribution station with a turboexpander installed parallel to pressure regulators. The turboexpander takes natural gas from the gas main to automatic pressure regulators (APRs). Through the regulating valve (RV), gas is fed to the turboexpander inlet. The exhausted (expanded) gas goes to the gas main after the APRs drop the gas pressure to the necessary level. Turboexpanders perform the same function. However, the latter may produce energy for gas distribution needs via an electric generator.

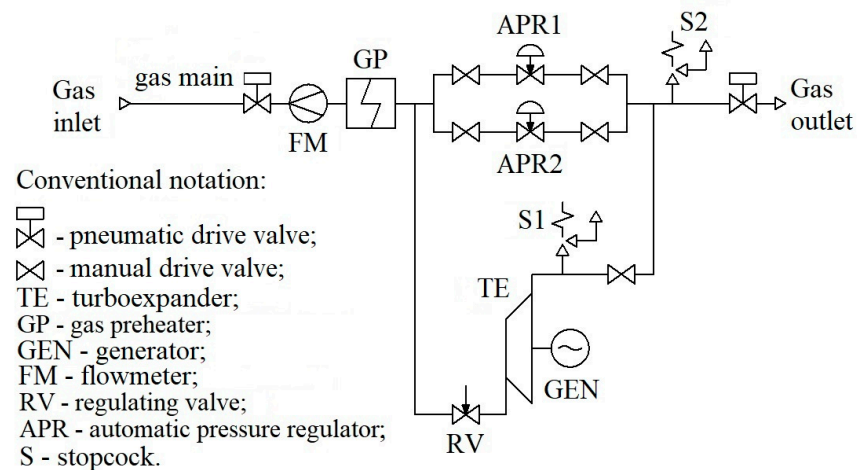


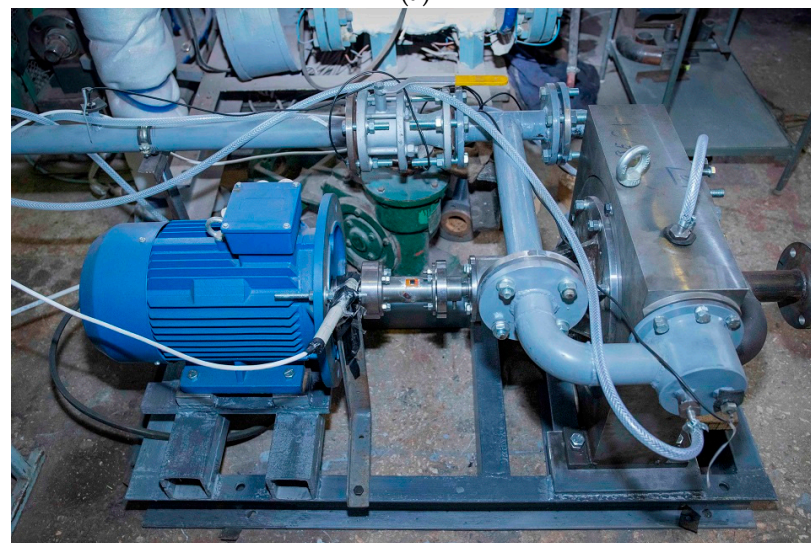
Figure 1. Turboexpander installation on gas distribution stations.

The turboexpander (turbogenerator) consists of an expander and an electric generator (Figure 2). As a turboexpander, we offer to apply a vortex expansion turbine. Figure 2 represents its construction with an external peripheral channel. The machine comprises a nozzle (1), a wheel (5), and a case (3) (with a working channel (2) and an outlet). There is a cutoff (6) between the nozzle and the outlet. The working substance goes through nozzle 1 (Figure 2) to the flow path, which consists of channel 2 of case 3 and the interblade channel (4) of the wheel (5). The wheel runs in the case with small radial and tip clearances. Gas leaves the flow path via the outlet. The potential energy of the compressed gas is converted into kinetic energy partially in the nozzle and partially in the case channel and the interblade wheel channels. Within the latter, particles move in different directions with a changing velocity. Finally, the blades force the wheel to run. Therefore, the gas flow interacts with the wheel blades, which convert kinetic energy into mechanical work on the turbine shaft. The circular substance velocity in the channel exceeds the circular wheel velocity. Within the flow path, gas particles move spirally from the inlet to outlet, pushing wheel blades via their energy. Such a vortex flow is basic for energy exchange

between channel gas and wheel blades. The more intensive it is, the more efficient the machine operates.



(a)



(b)

Figure 2. Cont.

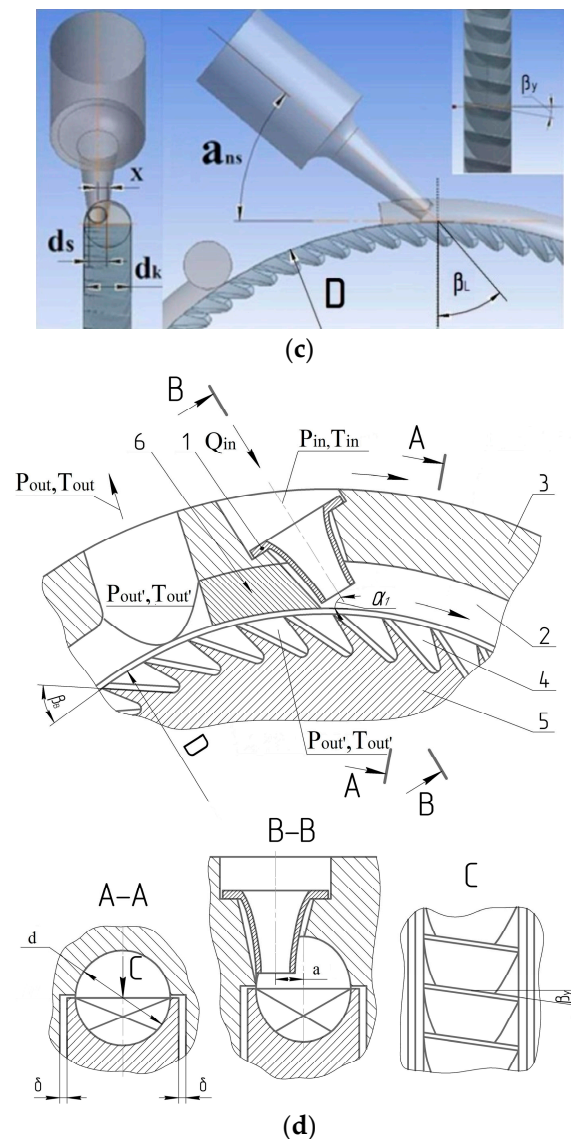


Figure 2. The turbogenerator 3D model based on a vortex turbine with the rotor location on the generator shaft (a), the turbogenerator prototype based on a vortex turbine (b), the vortex flow path 3D model (c), and the vortex turbine design (d) 1—nozzle, 2—working channel of the case, 3—housing, 4—interblade channels of the wheel, 5—wheel, and 6—cutoff.

Vortex equipment can be used to construct power-saving turbines. Their advantages include a simple design, low cost, stable performance, and high reliability, which helps to reduce risk factors. In contrast to axial and centripetal turbines, vortex expansion machines are easier and cheaper to manufacture. In the same conditions (capacity, size, and performance), vortex equipment avoids high revolution velocity as the principal disadvantage of axial, centrifugal, and jet-reactive turbines. Here, you do not need to apply reducers for pneumatic units. It decreases maintenance costs and increases machine reliability. Previously, research was conducted on one-channel and two-flow vortex expansion turbines with an external peripheral channel [3]. The latter is easy to construct, especially for multi-channel and multi-flow variants. This differs from vortex versions with side, side peripheral internal peripheral channels, etc. The advantages of vortex expansion machines allow manufacturing a simple and reliable turbine drive or turbogenerator with a 1–2-year payback. Such vortex equipment may be used up to 500 kW.

Literature Review

Within gas distribution stations and control points, pressure reduction may be complicated because of hydrate formation—a snow-like white crystal mass. The falling pressure and temperature drop the gas moisture capacity, which leads to hydrate formation [4]. Hydrates deposit on pipeline walls, orifice devices, pressure valves, etc. They not only obstruct gas measuring, but also cause emergencies (pipeline capacity decrease, hydrate plugs, and system damage). Hydrate removal is difficult: deposits can be solid, in hard-to-reach places. Additionally, the removal itself leads to harmful emissions. Even a full system shutdown may be required to remove hydrates. There are various ways to prevent hydrate formation. The most commonly used method is partial or general gas preheating. To complete this task, you should invest a lot of money. At the same time, gas preheating complicates gas distribution and emits combustion products into the atmosphere. Nevertheless, the necessary gas temperature is supported via direct or indirect preheating. A less efficient option is the local preheating of pressure regulator cases with electric ribbons. The advantage of the latter is that it is relatively low cost and nearby power sources. Also, we may inject methanol into the pipeline (although it is expensive to realize). Moreover, extra expenditure is required to protect the environment: methanol is a strong poison. To prevent hydrate formation, there are some specific techniques as well: the whole gas reduction node heating, the water jacket installation, etc. A safe reduction is offered for gas distribution stations to prevent hydrate formation via heat generators embedded into pressure regulators [5].

Currently, the hydrate formation problem is often considered for deep-water pipelines. Some ideas can be applied to gas distribution stations. Article [6] shows how the changing outer temperature of a pipeline wall impacts hydrate formation. Paper [7] reports on the carbon steel corrosion influence over the formation and dissociation of methane hydrate. Publication [8] discusses plug forecasts and anti-hydrate surfaces as another reasonable method to prevent hydrate deposits.

There are many works on the gas heating upgrade and its prevention (if turboexpanders are used). Article [9] involves the expansion machine being cold to lower the gas temperature at the inlet of both the compressor sections. Simultaneously, the compressed gas itself heats the turboexpander inlet gas with the extra power generation.

Within a single system, the wind energy, accumulator, solar power station, gas turbine, and recovery boiler are offered to be combined for the optimal planning of a cogeneration micro-network [10,11].

Paper [12] represents a pressure-decreasing system with a hybrid turboexpander and fuel cells. Here, molten carbonate generates extra power and partially heats gas before flowing to the turboexpander. Publication [13] considers the gas heating cost decrease via renewable energy sources. Heat pumps and various heat exchangers are offered for use.

Article [14] analyzes heat recovery on gas distribution stations and compares three types of expansion machines with different preheating principles. Low-expansion machines and gas heaters prove to be most efficient in heat recovery on gas distribution stations. However, the research does not discuss vortex turboexpanders. Paper [15] introduces a hybrid gas turbine with a solar gas preheating via a parabolic trough system. Such a system is compared with a more conventional solar unit.

Additionally, the excessive heating costs are proposed to drop via multi-stage expansion machines and heat pumps with a gas engine drive [16]. A hydrate prediction model has been created. It results in a significant preheating temperature decrease with economic and energetic benefits.

The authors of article [17] deal with increasing the energy efficiency of the new pump design for nuclear power plants, and the effect of impeller trimming on the energy efficiency of the counter-rotating pumping stage was published in [18].

Generally, there are different methods of alternative natural energy use on gas distribution stations. However, their application depends on the climatic conditions.

The results of experimental studies of a vortex expansion machine with a peripheral-side channel and a turbogenerator based on it are known [19]. During the pre-investigation of this turbine, the angle of inclination of the nozzles, the angle of cut of the nozzles, and the distance from the nozzles to the blades of the impeller changed. During the tests, the pressure at the turbine inlet and outlet and the rotor speed were changed. The excess pressure at the turbine inlet ranged from 1 to 5 kg/cm²; the turbine rotor speed was up to 3000 rpm. The highest efficiency value obtained during the tests was 25%. The plot of efficiency versus rotor speed and reduced circular speed was ascending and did not reach maximum values. This is due to the inability to get on the stand at speeds of more than 3000 rpm.

Article [3] represents calculations of a vortex turbine with an external peripheral channel, which was produced via the ANSYS software. Optimal parameters were obtained for three models of vortex turboexpanders with an external peripheral channel within the 2–6 pressure ratio range: relative nozzle diameter ($\bar{d}_n = d_n/d = 0.25 \div 0.4$); relative meridional section diameter of the turbine flow path ($\bar{d}_{fp} = d/D = 0.055 \div 0.065$); and circular wheel velocity $\bar{u} = 0.12 \div 0.2$. It is found that turbine efficiency can be more than 45% [3].

In order to obtain characteristics and confirm the adequacy of the results of the computational experiment, physical experiments were carried out at the stand created at the Department of Technical Thermophysics of Sumy State University [20]. A comparison of the results of a physical experiment with the results of studies in the ANSYS software complex showed their good coincidence [21].

Thus, there is a general problem of energy savings and a problem in increasing the reliability of gas distribution stations in the absence of electricity. These problems can be solved by the use of uninterruptible power sources, in particular, vortex turbogenerators, which work due to the energy of excess gas pressure, which is always present at the gas distribution station. The range of electrical power required for the needs of the gas distribution stations is 5–20 kW; this article examines turbogenerators with a capacity of 5, 10, and 20 kW. Having reviewed the sources, we can find many works about hydrate formation, including cases of gas pressure fall on distribution stations [4–8,16] and the use of turboexpanders and alternative solutions for obtaining electrical energy at the gas distribution station [9,11–14,16]. However, there are no articles about the varying outlet gas pressure influence on the entire regulatory range of this parameter change (0.3 ÷ 1.2 MPa) on the vortex turbogenerator values with a stable inlet gas temperature. The same concerns the gas preheating with a given outlet gas temperature. Therefore, our article comprises the following research steps:

1. A study of varying outlet gas pressure influences on the vortex turbogenerator values with a stable inlet gas temperature.
2. A study of varying outlet gas pressure influences on the vortex turbogenerator values with a stable outlet gas temperature.
3. A design of no-reduction turbogenerators with the vortex turbine rotor location on the generator shaft itself.
4. A calculation of the ratio between the turbogenerator gas flow and the distribution station gas flow.

2. Research Methodology

In the turboexpander, the gas cools down. Its temperature should be above -10 °C (in some cases, above 0 °C). Therefore, the gas must be heated with a loss of extra resources. Using preliminary calculations, we may determine those processes when it is possible to avoid excessive gas preheating for certain turboexpander indexes (efficiency and pressure ratio). Moreover, we can define the dependence of fuel-preheating gas on differential pressure, total technological gas consumption, and expansion efficiency. The energy expenditure for gas expansion is compared with that for pressure regulator throttling. To complete these calculations, we apply the software of the Sumy State University Department of Technical

Thermal Physics. In such a way, the available and useful capacity is assessed for the given turboexpander efficiency.

To design a turbogenerator based on vortex expansion machines for the throughput of 5000, 10,000 and 30,000 Nm³/h, we analyzed the inlet and outlet pressure as well as inlet temperature on gas distribution stations.

There is a technique to calculate vortex turbines by the Reynolds and Mach numbers. Through it, we can find the thermodynamic, gasodynamic, and energetic machine features as well as their dependence on the circular wheel velocity, efficiency, etc. This methodology produced a program based on Microsoft Excel.

The calculation algorithm is represented below.

The degree of pressure decrease in the vortex turbine:

$$\Pi_T = \frac{p_{in}}{p_{out}} \quad (1)$$

Adiabatic (isentropic) work of 1 gas kg expansion in the turbine:

$$h_s = \frac{k}{k-1} \cdot R \cdot T_{in} \cdot \left[1 - \left(\frac{p_{out}}{p_{in}} \right)^{\frac{k-1}{k}} \right] \quad (2)$$

The turbogenerator efficiency:

$$\eta_{TG} = \eta_T \cdot \eta_G \quad (3)$$

The capacity of turbogenerator drive:

$$N_{TG} = \frac{N}{\eta_G} \quad (4)$$

The adiabatic (isentropic) capacity of turbogenerator drive:

$$N_s = \frac{N_{TG}}{\eta_T} \quad (5)$$

Gas mass flow:

$$G = \frac{N_s}{h_s} \quad (6)$$

Outlet nozzle pressure:

$$p_N = p_{in} \cdot \left[1 - \frac{h_{S_N}(k-1)}{k \cdot R \cdot T_{in}} \right]^{\frac{k}{k-1}} \quad (7)$$

where h_{S_N} is the isoentropic work of 1 gas kg expansion in the nozzle:

$$h_{S_N} = \beta_s \cdot h_s \quad (8)$$

where β_s is the turbine activity coefficient.

Nozzle outlet gas velocity:

$$C_N = \varphi_N \cdot \sqrt{2 \cdot h_{S_N}} \quad (9)$$

where φ_N is the nozzle velocity coefficient.

Critical nozzle outlet velocity:

$$a_{cr} = \sqrt{\frac{2 \cdot k}{k+1} \cdot R \cdot T_{in}} \quad (10)$$

$$C_{cr} = a_{cr} \cdot \varphi_N \quad (11)$$

Dimensionless nozzle outlet velocity for actual expansion:

$$\lambda_N = \frac{C_N}{a_{cr}} \quad (12)$$

Function $q(\lambda_N)$:

$$q(\lambda_N) = \lambda_N \cdot \left[\frac{k+1}{2} \cdot \left(1 - \frac{k-1}{k+1} \cdot \lambda_N^2 \right) \right]^{\frac{1}{k-1}} \quad (13)$$

The square of the outlet nozzle section (in total, there are two nozzles):

$$f_N = \frac{G \cdot \sqrt{R \cdot T_{in}}}{2 \cdot B \cdot p_{in} \cdot q(\lambda_N)} \quad (14)$$

where

$$B = \sqrt{k \cdot \left(\frac{2}{k+1} \right)^{\frac{k+1}{k-1}}} \quad (15)$$

Diameter of outlet nozzle section:

$$d_N = \sqrt{\frac{4 \cdot f_N}{\pi}} \quad (16)$$

Square of critical nozzle section (in total, there are two nozzles):

$$f_{cr} = \frac{G \cdot \sqrt{R \cdot T_{in}}}{2 \cdot B \cdot p_{out}} \quad (17)$$

Critical nozzle diameter:

$$d_{cr} = \sqrt{\frac{4 \cdot f_{cr}}{\pi}} \quad (18)$$

The diameter of the flow path meridional section:

$$d_{fp} = \frac{d_N}{d_N} \quad (19)$$

Outer wheel diameter:

$$D = \frac{d_{fp}}{d_{fp}} \quad (20)$$

Turbine outlet temperature:

$$T_{out} = T_{in} \left[1 - \eta_T \left(1 - \Pi^{\frac{1-k}{k}} \right) \right] \quad (21)$$

Calculation of the inlet pipe.

Pipe cross-sectional area:

$$f_{in} = \frac{G}{C_p \cdot \rho_{in}} \quad (22)$$

where C_p is the pipe gas velocity, ρ_{in} is the gas density for the turbine inlet:

$$\rho_{in} = \frac{p_{in}}{R \cdot T_{in}} \quad (23)$$

Inlet pipe diameter:

$$d_{in} = \sqrt{\frac{4 \cdot f_{in}}{\pi}} \quad (24)$$

Calculation of the outlet pipe.

Pipe cross-sectional area:

$$f_{out} = \frac{G}{C_p \cdot \rho_{out}} \quad (25)$$

where ρ_{out} is the gas density for the turbine outlet:

$$\rho_{out} = \frac{p_{out}}{R \cdot T_{out}} \quad (26)$$

Outlet pipe diameter:

$$d_{out} = \sqrt{\frac{4 \cdot f_{out}}{\pi}} \quad (27)$$

3. Results

3.1. Turbogenerator Calculations without the Outlet Gas Distribution Temperature

We calculated nine turbogenerator variants for the needs of the gas distribution stations based on vortex expansion machines. The initial data are indicated in Table 1. For each outlet gas distribution pressure (0.3, 0.6, and 1.2 MPa), turbogenerators with the capacity of 5, 10, and 20 kW were estimated.

Table 1. The initial data for turbogenerator calculations.

Inlet pressure, P_{in} , MPa	2.5
Inlet temperature, T_{in} , K	278
Gas constant, R , J/(kg·K)	506
Adiabatic index, k	1.3
Outlet pressure, P_{out} , MPa	0.3; 0.6; 1.2
Turbogenerator electric capacity, N , kW	5; 10; 20

The calculations define the geometric, thermodynamic, gasodynamic, and energetic features of the turbogenerators (Table 2).

For each N value of the turbogenerator electric capacity, we produced the P_{out} diagrams against the following:

- Gas mass flow through the turbogenerator Q_T (Figure 3);
- The correlation between gas mass flow through the turbogenerator and that through the gas distribution station Q_T/Q_{GDS} : 5000 Nm³/h (GDS 5, Figure 4); 10,000 Nm³/h (GDS 10, Figure 5); and 30,000 Nm³/h (GDS 30, Figure 6);
- The outer wheel diameter of the vortex expansion machine D (Figure 7).

We see that the P_{out} increase from 0.3 to 1.2 MPa leads to the following:

1. The Q_T rose from 270.1 to 672.9 Nm³/h (turbogenerator electric capacity $N = 5$ kW). It makes the following:
 - 5 to 8% of the gas mass flow for the GDS throughput of 5000 Nm³/h;
 - 2.5 to 6.5% of the gas mass flow for the GDS throughput of 10,000 Nm³/h;
 - 1 to 2.2% of the gas mass flow for the GDS throughput of 30,000 Nm³/h.
2. The Q_T rises from 535.3 to 1335.9 Nm³/h (turbogenerator electric capacity $N = 10$ kW). It makes the following:
 - 10 to 20% of the gas mass flow for the GDS throughput of 5000 Nm³/h;
 - 5 to 13% of the gas mass flow for the GDS throughput of 10,000 Nm³/h;

- 1.8 to 4.5% of the gas mass flow for the GDS throughput of 30,000 Nm³/h.
3. The Q_T rises from 1070.7 to 2657.0 Nm³/h (turbogenerator electric capacity $N = 20$ kW). It makes the following:
 - 22 to 53% of the gas mass flow for the GDS throughput of 5000 Nm³/h;
 - 11 to 26.5% of the gas mass flow for the GDS throughput of 10,000 Nm³/h;
 - 3.6 to 8.9% of the gas mass flow for the GDS throughput of 30,000 Nm³/h.
 4. The D rises from 0.15 to 0.22 m ($N = 5$ kW); from 0.21 to 0.31 m ($N = 10$ kW); and from 0.29 to 0.44 m ($N = 20$ kW).

Concerning the highest turbine efficiency, the optimal range of circular wheel velocity for the vortex equipment is $\bar{u} = 0.12 \div 0.2$ [1,3]. This is one of the main dimensionless parameters in the theory and practice of turboexpanders. It relates geometrical size (outer wheel diameter) to the rotor revolutions, thermodynamic features of the inlet and outlet gas flow, and physical properties of the working substance:

$$\bar{u} = \frac{u}{\sqrt{2h_s}} = \frac{\pi D n_T}{60 \cdot \sqrt{\frac{2k}{k-1} RT_{in} \left[1 - \left(\frac{p_{in}}{p_{out}} \right)^{\frac{k-1}{k}} \right]}} \quad (28)$$

where h_s is the isentropic expansion of 1 kg gas in the turbine (specific work), J/kg, u is circular wheel velocity (outer diameter), m/s, and n_T is the frequency of rotor revolutions per minute, rpm.

Table 2. Calculation results.

$P_{in} = 2.5$ MPa; $T_{in} = 278$ K									
	$P_{out} = 0.3$ MPa			$P_{out} = 0.6$ MPa			$P_{out} = 1.2$ MPa		
N , kW	5	10	20	5	10	20	5	10	20
G , kg/s ¹	0.055	0.109	0.218	0.076	0.151	0.304	0.137	0.272	0.541
Q_T , Nm ³ /h ²	270.1	535.3	1070.7	373.3	741.6	1493.0	672.9	1335.9	2657.0
d_n , m ³	0.0031	0.0044	0.0062	0.0034	0.0048	0.0067	0.0046	0.0065	0.0092
d_n/d ⁴					0.35				
d , m ⁵	0.0089	0.0125	0.0176	0.0096	0.0136	0.0192	0.0132	0.0186	0.0262
d/D ⁶					0.6				
D , m ⁷	0.15	0.21	0.29	0.16	0.23	0.32	0.22	0.31	0.44
d_{in} , m ⁸	0.010	0.014	0.020	0.012	0.016	0.023	0.016	0.022	0.031
d_{out} , m ⁹	0.026	0.037	0.052	0.022	0.031	0.044	0.022	0.031	0.043
T_{out} , K ¹⁰		231			244			259	

¹ Gas mass flow at the vortex expansion machine inlet, G , kg/s. ² Gas at the vortex expansion machine inlet for normal physical conditions, Q_T , Nm³/h. ³ The diameter of outlet nozzle section, d_n , m; ⁴ Relative nozzle diameter, d_n/d . ⁵ The diameter of flow path meridional section, d , m; ⁶ The relative diameter of the flow path meridional section, d/D (Figure 2); ⁷ Outer wheel diameter, D , m; ⁸ Inlet pipe diameter, d_{in} , m; ⁹ Outlet pipe diameter, d_{out} , m; and ¹⁰ Temperature at the vortex expansion machine outlet, T_{out} , K.

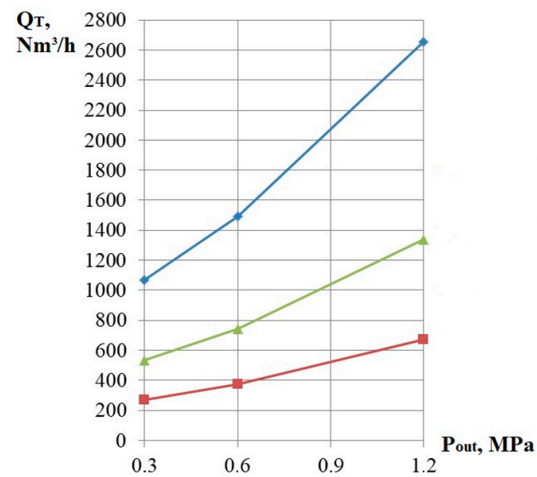


Figure 3. Gas mass flow Q_T against outlet pressure P_{out} for turbogenerator electric capacity $N = 20$ kW, $N = 10$ kW, and $N = 5$ kW.

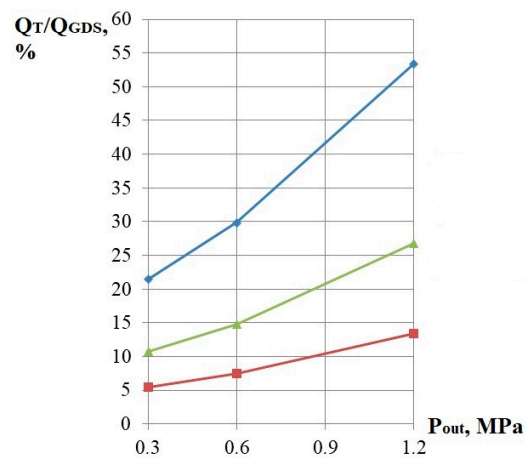


Figure 4. The gas mass flow correlation Q_T/Q_{GDS} on GDS 5 against outlet pressure P_{out} for turbogenerator electric capacity $N = 20$ kW, $N = 10$ kW, and $N = 5$ kW.

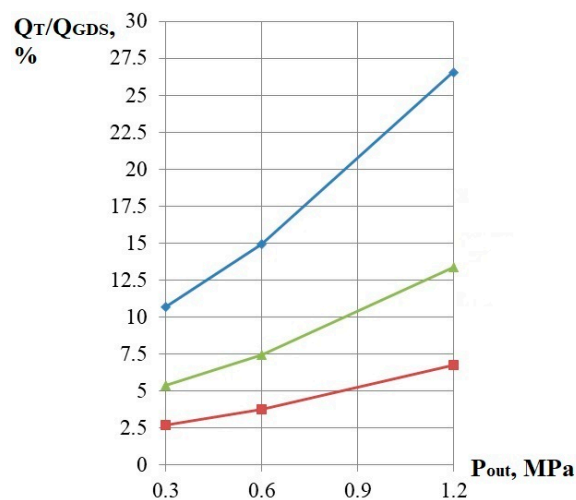


Figure 5. The gas mass flow correlation Q_T/Q_{GDS} on GDS 10 against outlet pressure P_{out} for turbogenerator electric capacity $N = 20$ kW, $N = 10$ kW, and $N = 5$ kW.

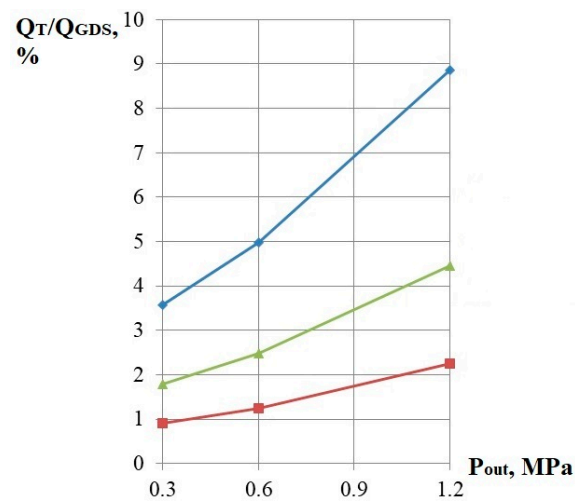


Figure 6. The gas mass flow correlation Q_T/Q_{GDS} on GDS 30 against outlet pressure P_{out} for turbogenerator electric capacity $N = 20$ kW, $N = 10$ kW, and $N = 5$ kW.

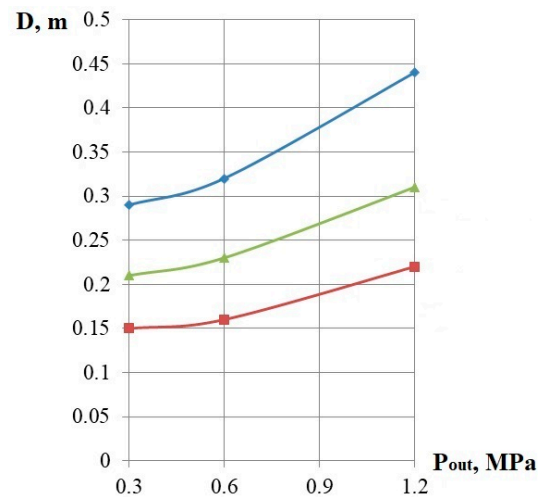


Figure 7. Wheel diameter D against outlet pressure P_{out} for turbogenerator electric capacity $N = 20$ kW, $N = 10$ kW, and $N = 5$ kW.

For $\bar{u} = 0.15$ and the given geometric parameters (Table 2), we obtain the rotor revolutions (Table 3).

Table 3. Rotor revolutions for $\bar{u} = 0.15$.

	$P_{in} = 2.5$ MPa; $T_{in} = 278$ K								
	$P_{out} = 0.3$ MPa			$P_{out} = 0.6$ MPa			$P_{out} = 1.2$ MPa		
	N , kW	5	10	20	5	10	20	5	10
n_T , rpm	13,330	9460	6710	10420	7400	5240	5680	4300	2860

Table 3 produces a diagram of the rotor revolutions n_T against the outlet pressure P_{out} (Figure 8).

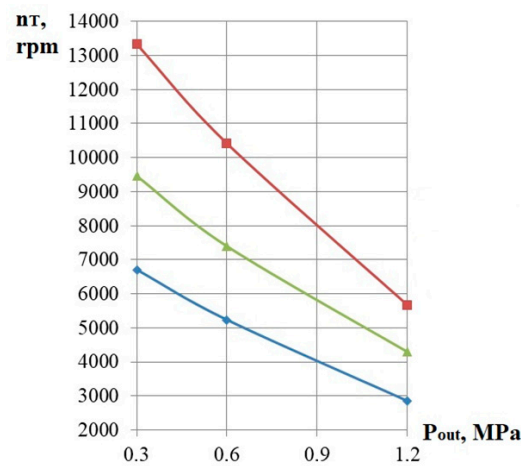


Figure 8. Wheel revolutions per minute n_T against outlet pressure P_{out} for turbogenerator electric capacity — $N = 20$ kW, — $N = 10$ kW, and — $N = 5$ kW (circular velocity $\bar{u} = 0.15$).

The above-mentioned indicates that the rotor revolutions within the highest turbine efficiency range from 2860 to 13300 rpm. In the case of 3000 rpm, we can apply a turbogenerator with a rotor location on the electric generator shaft itself. Such a design is possible only for $P_{out} = 1.2$ MPa; $N = 20$ kW with a slight (up to 5%) decrease in the outer wheel diameter. The eight additional turbogenerator versions exceed 3000 rpm.

To reduce the rotor revolutions, we adjust the relative nozzle diameter ($\bar{d}_n = d_n/d = 0.25 \div 0.4$), the relative diameter of the flow path meridional section ($\bar{d}_{fp} = d/D = 0.055 \div 0.065$), and the circular wheel velocity to the highest vortex turbine efficiency. The calculation results are shown in Table 4.

Table 4. Refined calculation results.

Variant	$P_{in} = 2.5$ MPa; $T_{in} = 278$ K								
	$P_{out} = 0.3$ MPa			$P_{out} = 0.6$ MPa			$P_{out} = 1.2$ MPa		
	1	2	3	4	5	6	7	8	9
N , kW	5	10	20	5	10	20	5	10	20
G , kg/s	0.055	0.109	0.218	0.076	0.151	0.304	0.137	0.272	0.541
Q_T , Nm ³ /h	270.1	535.3	1070.7	373.3	741.6	1493.0	672.9	1335.9	2657.0
d_n , m	0.0031	0.0044	0.0062	0.0034	0.0048	0.0067	0.0046	0.0065	0.0092
d_n/D	0.25	0.25	0.25	0.25	0.25	0.25	0.25	0.275	0.365
d , m	0.0124	0.0175	0.0247	0.0135	0.0191	0.0269	0.0185	0.0236	0.0252
d/D	0.055	0.055	0.055	0.055	0.055	0.055	0.055	0.056	0.06
D , m	0.23	0.32	0.45	0.25	0.35	0.49	0.34	0.42	0.42
\bar{u}	0.140	0.140	0.140	0.140	0.140	0.131	0.121	0.150	0.150
n_T , rpm	8150	5777	4096	6365	4515	3000	3000	3000	3000
T_{out} , K		231			244			259	

The obtained data produce two diagrams. Firstly, the rotor revolutions n_T against the outlet pressure P_{out} (Figure 9). Secondly, the outer wheel diameter D against the outlet pressure P_{out} (Figure 10).

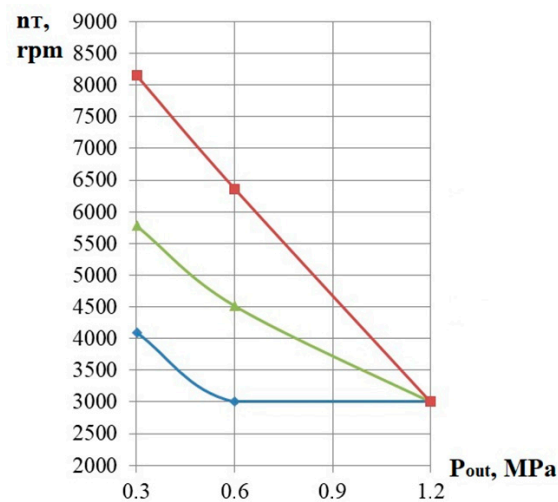


Figure 9. Wheel revolutions per minute n_T ($\bar{u} = 0.12 \div 0.15$) against outlet pressure P_{out} for turbogenerator electric capacity — $N = 20$ kW, $N = 10$ kW, and $N = 5$ kW.

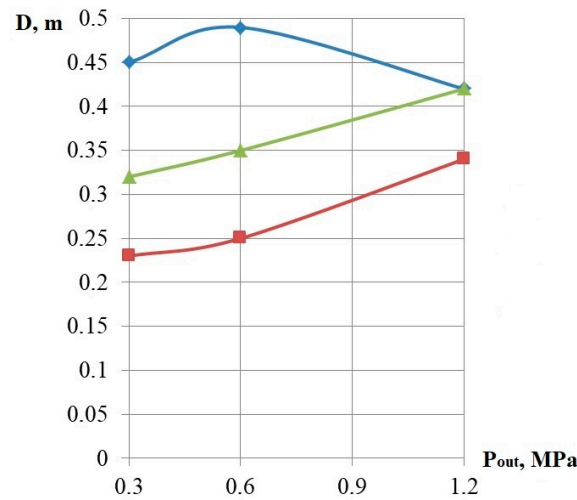


Figure 10. Wheel diameter D ($\bar{u} = 0.12 \div 0.15$) against outlet pressure P_{out} for turbogenerator electric capacity — $N = 20$ kW, $N = 10$ kW, and $N = 5$ kW.

The above-mentioned information indicates that there are four possible turbogenerator versions with 3000 rpm (rotor location on the electric generator shaft itself). For the outer wheel diameter D , we can have such changes:

1. Version 9 ($P_{out} = 1.2$ MPa, $N = 20$ kW): decrease from 0.44 m (Table 2) to 0.42 m (Table 4). Here, the rotor revolutions may be raised while the outer wheel diameter is dropped.
2. Version 8 ($P_{out} = 1.2$ MPa, $N = 10$ kW): increase from 0.31 m to 0.42 m.
3. Version 7 ($P_{out} = 1.2$ MPa, $N = 5$ kW): increase from 0.22 m to 0.34 m.
4. Version 6 ($P_{out} = 0.6$ MPa, $N = 20$ kW): increase from 0.32 m to 0.49 m.

Considering the outer wheel diameter of versions 6, 7, and 8, the final decision on the turbogenerator design must be made according to additional technical and economic calculations.

In other versions, a drive should be used for decreasing the rotor revolutions to shaft revolutions of the electric generator.

3.2. Influence of the GDS Outlet Gas Temperature on the Turbogenerator Parameters

The research methodology for vortex expansion machines includes a formula to calculate the turbine outlet gas temperature (21). Using this equation, we performed

corresponding calculations. Figure 11 shows the turbine outlet gas temperature t_{out} against the efficiency η_T , and the turbine pressure falls by degree Π_T . It concerns the ideal gas with the turbine inlet temperature $T_{in} = 298 \text{ K}$ ($t_{out} = 25 \text{ }^\circ\text{C}$).

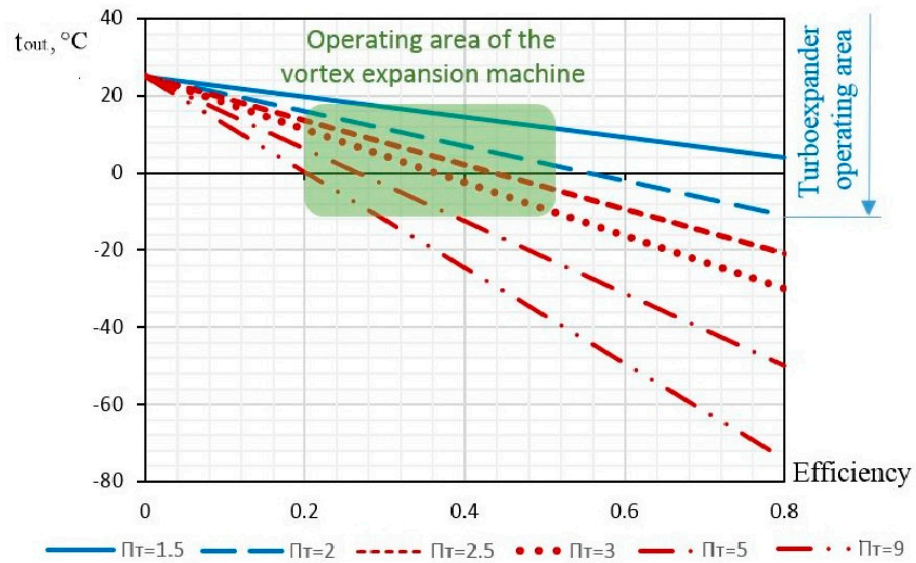


Figure 11. Turbine outlet gas temperature t_{out} against efficiency η_T and turbine pressure fall degree Π_T .

As we can see, the turbine outlet gas temperature depends significantly on its efficiency and pressure fall degree: the higher the efficiency and pressure fall degree is, the lower the outlet temperature is. The vortex turbine efficiency ranges from 0.2 to 0.48. Figure 11 represents the vortex turbine operating area at the outlet gas temperature over 263 K ($-10 \text{ }^\circ\text{C}$).

According to the obtained results, we made diagrams of the turbine outlet gas temperature t_{out} against the turbine inlet gas temperature t_{in} for the machine efficiency 0.2, 0.4, and 0.6 and the pressure fall degree $\Pi_T = 2$ (Figure 12). The outlet temperature over 263 K ($-10 \text{ }^\circ\text{C}$) should match the inlet temperature over $7 \text{ }^\circ\text{C}$ with an efficiency of 0.4 and over $16 \text{ }^\circ\text{C}$ with an efficiency of 0.6. The outlet temperature over 273 K ($0 \text{ }^\circ\text{C}$) should match the inlet temperature over $8 \text{ }^\circ\text{C}$ with an efficiency of 0.2, over $18 \text{ }^\circ\text{C}$ with an efficiency of 0.4, and over $27 \text{ }^\circ\text{C}$ with an efficiency of 0.6.

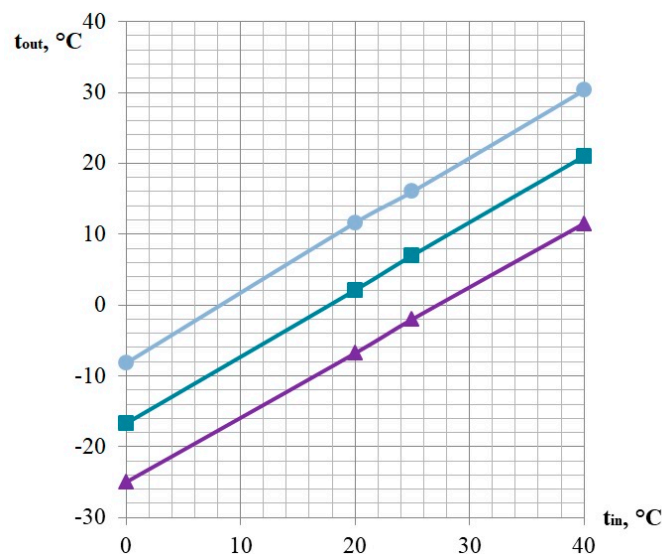


Figure 12. The turbine outlet gas temperature t_{out} against the turbine inlet gas temperature t_{in} for the machine efficiency $\eta_T = 0.2$; $\eta_T = 0.4$; and $\eta_T = 0.6$, and the pressure fall degree $\Pi_T = 2$.

Figure 13 reflects the turbine outlet gas temperature t_{out} against the efficiency η_T and the turbine pressure fall degree $\Pi_T = 2$ and $\Pi_T = 5$ with the inlet pressure $P_{in} = 2.5$ MPa and temperature $T_{out} = 298$ K ($t_{in} = 25$ °C). This concerns the ideal and real gas (based on the natural gas diagram). In the case of the efficiency 0, the real gas throttling from $P_{in} = 2.5$ MPa to $P_{out} = 1.25$ MPa ($\Pi_T = 2$) causes the temperature to decrease by 7 °C. Such a temperature difference practically does not depend on the turbine efficiency. The real gas throttling from $P_{in} = 2.5$ MPa to $P_{out} = 0.5$ MPa ($\Pi_T = 5$) causes the temperature to decrease by 10 °C. This temperature difference falls to 4 °C if the turbine efficiency rises to 0.8.

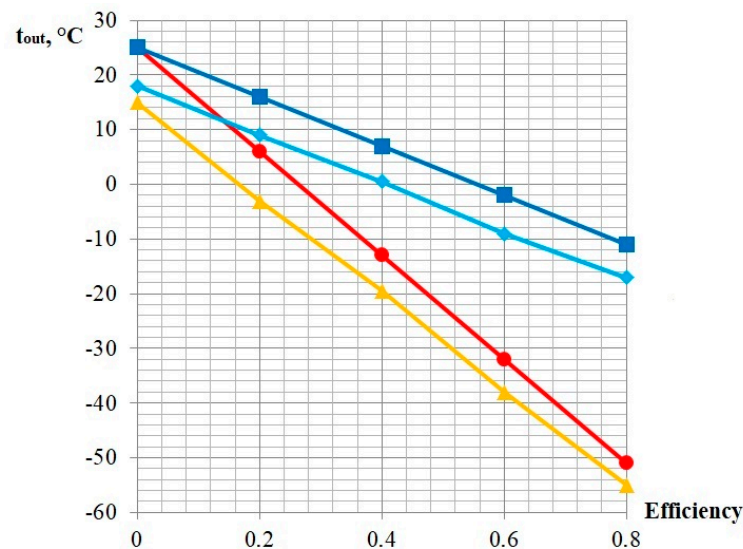


Figure 13. Outlet turbine temperature t_{out} against efficiency with various pressure fall degrees: \blacksquare $\Pi_T = 2$ (ideal gas), \blacklozenge $\Pi_T = 5$ (real gas, $P_{in} = 2.5$ MPa), \bullet $\Pi_T = 5$ (ideal gas), and \blacktriangle $\Pi_T = 5$ (real gas, $P_{in} = 2.5$ MPa).

Therefore, taking into account the real gas properties, the design outlet temperature decreases in contrast to the ideal gas. This restricts the turbogenerator operating area shown in Figure 11.

To prevent hydrate formation in the case of gas throttling and expanding, it is often preheated with natural gas. According to Ukrainian standards, the GDS outlet gas temperature must be 273 K (0 °C). The calculations included in this article in Section 3.1 do not include gas preheating with $P_{in} = 2.5$ MPa, $T_{in} = 278$ K, and turbine efficiency $\eta_T = 0.44$. Simultaneously, $P_{out} = 0.3$ MPa for $T_{out} = 231$ K; $P_{out} = 0.6$ MPa for $T_{out} = 244$ K; $P_{out} = 1.2$ MPa and for $T_{out} = 259$ K. Since all the obtained values are under 273 K, gas preheating is required to raise the turbine outlet gas temperature.

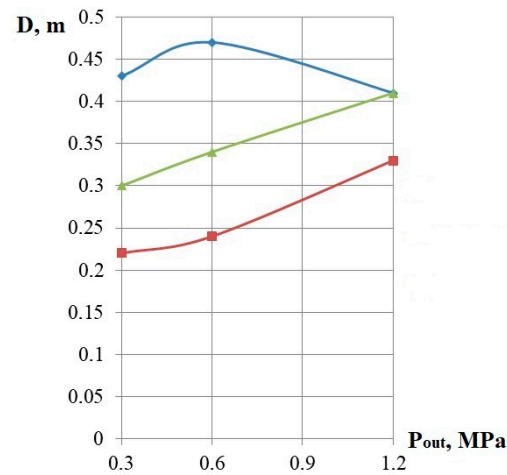
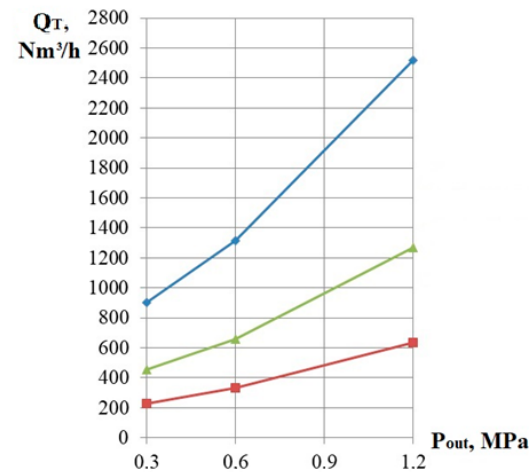
We performed new calculations for vortex expansion turbogenerators. Conditions: $P_{in} = 2.5$ MPa, $T_{out} = 273$ K for electric capacity $N = 5, 10,$ and 20 kW, and $P_{out} = 0.3, 0.6,$ and 1.2 MPa. We recognize here the turbine inlet gas temperature T_{in} as a design parameter. The calculation results for the turbine inlet gas preheating are indicated in Table 5.

Tables 4 and 5 show that the lower the outlet pressure is (high pressure difference), the higher the inlet temperature is (for $T_{out} = 273$ K). Gas inlet preheating (the difference between preheated and non-preheated gas with $T_{in} = 278$ K) is 51 °C for $P_{out} = 0.3$ MPa, 34 °C for $P_{out} = 0.6$ MPa, and 15 °C for $P_{out} = 1.2$ MPa.

Consequently, we produce diagrams of the outer wheel diameter D (Figure 14), the turbine gas flow Q_T (Figure 15), and the ratio between preheated and non-preheated gas mass flow Q_h/Q_T (Figure 16) against the outlet pressure P_{out} .

Table 5. Final calculation results for $T_{out} = 273$ K.

	$P_{in} = 2.5$ MPa; $T_{in} = 278$ K								
	$P_{out} = 0.3$ MPa			$P_{out} = 0.6$ MPa			$P_{out} = 1.2$ MPa		
	5	10	20	5	10	20	5	10	20
N , kW									
G , kg/s	0.047	0.093	0.184	0.068	0.135	0.268	0.130	0.258	0.513
Q_T , Nm ³ /g	228.5	454.4	903.7	332.3	660.7	1314.1	637.2	1267.2	2520.0
d_n , m	0.0030	0.0042	0.0059	0.0033	0.0046	0.0065	0.0046	0.0064	0.0091
d_n/D	0.25	0.25	0.25	0.25	0.25	0.25	0.25	0.28	0.37
d , m	0.0119	0.0168	0.0236	0.0131	0.0185	0.0261	0.0182	0.0230	0.0246
d/D	0.055	0.055	0.055	0.055	0.055	0.055	0.055	0.056	0.06
D , m	0.22	0.3	0.43	0.24	0.34	0.47	0.33	0.41	0.41
D_{in} , m	0.010	0.014	0.020	0.012	0.016	0.023	0.016	0.022	0.031
D_{out} , m	0.026	0.037	0.052	0.022	0.031	0.044	0.022	0.031	0.043
T_{in} , K		329			312			293	
\bar{u}	0.14	0.14	0.14	0.14	0.14	0.12	0.12	0.144	0.144
n_T , rpm	9245	6555	4650	6940	4924	3000	3000	3000	3000

**Figure 14.** Outer wheel diameter D against outlet pressure P_{out} for turbogenerator electric capacity $N = 20$ kW, $N = 10$ kW, and $N = 5$ kW ($T_{out} = 273$ K).**Figure 15.** Turbine gas flow Q_T against outlet pressure P_{out} for turbogenerator electric capacity $N = 20$ kW, $N = 10$ kW, and $N = 5$ kW ($T_{out} = 273$ K).

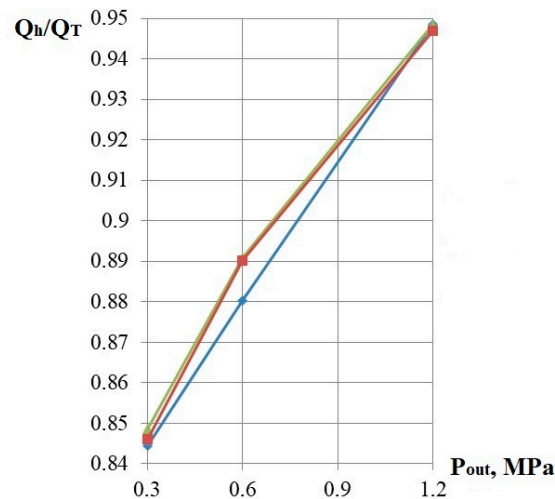


Figure 16. The ratio between preheated and non-preheated gas mass flow Q_h/Q_T against the outlet pressure P_{out} for turbogenerator electric capacity — $N = 20$ kW, $N = 10$ kW, and $N = 5$ kW ($T_{out} = 273$ K).

According to Tables 4 and 5, as well as Figures 14–16, the preheated inlet gas and outlet pressure drop lead to a significant decrease in gas mass flow through the turbine (up to 15%, Figure 15). At the same time, there is a slight decrease in the outer wheel diameter (up to 4%, Figures 10 and 14).

4. Discussion

In this study, various calculations of vortex expansion machines for turbogenerators of gas distribution stations with powers of 5, 10, and 20 kW were carried out at inlet pressure $P_{in} = 2.5$ MPa and outlet pressures $P_{out} = 0.3, 0.6,$ and 1.2 MPa, without taking into account the preheating of the gas upstream of the turbine at the specified temperature at the inlet of the turbine $T_{in} = 278$ K.

From the results of the studies (Table 6), it was found that when the pressure at the turbine outlet increases from 0.3 to 1.2 MPa, the following parameters will increase:

- Required mass flow of the gas through the turbine by 2.5 times for the post-power generator;
- Turbine outlet temperatures by 1.12 times (from 231 K to 259 K) depending on the turbine outlet pressure.
- The outer diameter of the impeller by 2.93 times, depending on the power of the turbine generator.

Table 6. Final calculation results for $T_{in} = 278$ K.

Option No	$P_{out} = 0.3$ MPa			$P_{out} = 0.6$ MPa			$P_{out} = 1.2$ MPa		
	1	2	3	4	5	6	7	8	9
$N, \text{ kW}$	5	10	20	5	10	20	5	10	20
$G, \text{ kg/s}$	0.055	0.109	0.218	0.076	0.151	0.304	0.137	0.272	0.541
$Q_T, \text{ Nm}^3/\text{h}$	270.1	535.3	1070.7	373.3	741.6	1493.0	672.9	1335.9	2657.0
$D, \text{ m}$	0.15	0.21	0.29	0.16	0.23	0.32	0.22	0.31	0.44
$T_{out}, \text{ K}$		231			244			259	

The reasons for differences in calculation results by variant are related to the following:

1. Increasing the required power of the turbine generator from 5 kW to 10 kW (two times) at a constant pressure at the turbine outlet of 0.3 MPa for option 2 compared to option

1 leads to a practically proportional increase in the required gas flow rate at the turbine inlet. Since the thermodynamic parameters at the inlet and outlet of the turbine are the same in these embodiments, the velocity and gas density at the outlet of the nozzle remain constant, and the area of the outlet section of the nozzle increases by 2 times, which leads to an increase in the diameter of the outlet section of the nozzle by 1.4 times. At the same values of relative nozzle diameter and relative meridional cross-section diameter of the turbine flow part, the outer diameter of the impeller also increases by 1.4 times.

2. The same reasons lead to the same changes in parameters when increasing power from 10 kW (option 2) to 20 kW (option 3). For option 3, the gas mass flow rate increases by a factor of four and the diameter by a factor of two compared to option 1.
3. An increase in the turbine outlet pressure from 0.3 MPa to 0.6 MPa (two times) for variants of turbine generators 4, 5, and 6 compared to variants 1, 2, and 3 leads to a decrease in pressure reduction in the vortex turbine by two times, and the adiabatic work of expansion of 1 kg of gas in a turbine by 1.38 times, according to Equation (2). Therefore, to provide the same power of 5 kW at the turbine outlet pressure of 0.6 MPa (option 4), compared to the turbine generator of the same power of 5 kW, but at the turbine outlet pressure of 0.3 MPa (option 1), it is necessary, according to Equation (6), to increase the gas flow rate at the turbine inlet by 1.38 times. In addition, thermodynamic parameters in the turbine flow part are changed and pressure differences between the nozzle and impeller are redistributed, which leads to a decrease in pressure difference on the nozzle and speed at the nozzle outlet, but the gas density at the nozzle outlet increases. As a result, we find that it is necessary to increase the area and, accordingly, the diameter of the outlet section of the nozzle, which leads, at the same values of the relative diameter of the nozzle and the relative diameter of the meridional section of the flow part of the turbine, to an increase in the outer diameter of the impeller from 0.15 m to 0.16 m.
4. The reasons for differences in calculation results in case 5 compared to case 4 are similar to cases 2 and 1.
5. The reasons for differences in calculation results in case 6 compared to case 5 are similar to cases 3 and 2.
6. An increase in the turbine outlet pressure from 0.6 MPa to 1.2 MPa (2 times) for turbine generator variants 7, 8, and 9 compared to variants 4, 5, and 6 leads to a decrease in the degree of pressure reduction in the vortex turbine by 2 times and an adiabatic work of expansion of 1 kg of gas in the turbine by 1.8 times, according to Equation (2). Therefore, to provide the same power of 5 kW at the turbine outlet pressure of 1.2 MPa (option 7) compared to the turbine generator of the same power of 5 kW, but at the turbine outlet pressure of 0.6 MPa (option 4), according to Equation (6), it is necessary to increase the gas flow rate at the turbine inlet by 1.8 times. As a result of the redistribution of pressure differences between the nozzle and impeller, the velocity and gas density at the outlet of the nozzle change accordingly. As a result, we have an increase in the area and, accordingly, the diameter of the outlet section of the nozzle and, at the same values of the relative diameter of the nozzle and the relative diameter of the meridional section of the turbine flow part, an increase in the outer diameter of the impeller from 0.16 m to 0.22 m.
7. The reasons for the differences in the calculation results in case 8 compared to case 7 are similar to cases 2 and 1.
8. The reasons for differences in calculation results in case 6 compared to case 5 are similar to cases 3 and 2.

The gas flow rate Q_T , Nm^3/h is changed as follows:

- (a) For the turbogenerator with power $N = 5$ kW-increasing from 270.1 to 672.9 Nm^3/h , which is:
 - 5 to 8% of the gas mass flow for the GDS throughput of 5000 Nm^3/h ;
 - 2.5 to 6.5% of the gas mass flow for the GDS throughput of 10,000 Nm^3/h ;

- 1 to 2.2% of the gas mass flow for the GDS throughput of 30,000 Nm³/h.
- (b) For the turbogenerator with power $N = 10$ kW-increasing from 535.3 to 1335.9 Nm³/h, which is:
 - 10 to 20% of the gas mass flow for the GDS throughput of 5000 Nm³/h;
 - 5 to 13% of the gas mass flow for the GDS throughput of 10,000 Nm³/h;
 - 1.8 to 4.5% of the gas mass flow for the GDS throughput of 30,000 Nm³/h.
- (c) For the turbogenerator with power $N = 20$ kW-increasing from 1070.7 to 2657.0 Nm³/h, which is:
 - 22 to 53% of the gas mass flow for the GDS throughput of 5000 Nm³/h;
 - 11 to 26.5% of the gas mass flow for the GDS throughput of 10,000 Nm³/h;
 - 3.6 to 8.9% of the gas mass flow for the GDS throughput of 30,000 Nm³/h.
- (d) The outer diameter of the impeller of the vortex turbine D is increased for a turbine generator with a power of $N = 5$ kW from 0.15 m to 0.22 m (1.47 times); for a turbine generator with power $N = 10$ kW from 0.21 to 0.31 m (1.48 times); for a high-power turbogenerator $N = 20$ kW from 0.29 to 0.44 m (1.52 times).

As a result of calculations at constant gas temperatures at the outlet of the turbine $T_{out} = 273$ K and variable inlet temperatures, depending on the gas pressure at the outlet of the gas distribution station, it is obtained that this temperature is achieved by heating the gas before the turbine generator, which leads to a slight decrease in the diameter of the impeller (by 1–4%) and a significant decrease in gas flow through the turbine generator (by 5 ÷ 15%).

Gas can be preheated with the pipeline gas. Therefore, the use of alternative power resource-saving technologies is desirable. Additionally, the turbogenerator energy can be applied.

Thus, the ratio of flow through the turbine generator to gas flow through the gas distribution station in the studied ranges of pressure change at the turbine outlet is 0.3 ÷ 2 MPa; the power of the turbogenerators 5 ÷ 20 kW and the capacity of gas distribution stations 5000 ÷ 30000 Nm³/h, which varies in the range 1 ÷ 53%.

For an optimal performance of the vortex expansion machine, we should adjust the wheel revolution frequency to 3000 rpm. This simplifies the turbogenerator design: the turbine wheel may be installed on the generator shaft since there is no need for a lowering drive to connect the turbine shaft to the generator. It also reduces the machine payback, simplifies its operation, etc. Such an opportunity is provided for turbogenerators with $P_{out} = 0.6$ MPa and $N = 20$ kW; $P_{out} = 1.2$ MPa and $N = 5, 10, 20$ kW.

5. Conclusions

In this article, we have studied how gas pressure and gas preheating influence turbogenerator parameters for electricity generation at gas distribution stations from the gas overpressure energy. The novelty is in the fact that this is a study of varying outlet gas pressures' influence on the vortex turbogenerator values with a stable inlet gas temperature and changeable outlet temperature depending on the gas pressure of the distribution station outlet. The same finding has been studied with a stable outlet gas temperature and changeable inlet temperature depending on the gas pressure of the distribution station outlet.

The discussed results show that it is reasonable to use vortex expansion machines to construct turbogenerators for gas distribution stations, which is the main contribution of the presented research. As a topic for future research, we regard techniques to upgrade the flow path efficiency of vortex expansion machines. Nevertheless, today's introduction of these power-saving turbogenerators may significantly raise economic benefits and ensure energy independence or the autonomy of gas distribution stations.

Thus, for the first time, the main parameters of vortex turbogenerators for the needs of gas distribution stations were obtained in the work throughout the regulatory range of gas pressure changes at the outlet of the gas distribution station (0.3–1.2 MPa). The

investigated capacities of turbogenerators of 5, 10, or 20 kW correspond to the range of electric capacities required for the needs of the gas distribution stations. It was investigated how much of the gas goes through the turbine generator in relation to the gas flow rate through the GDS as a whole for the GDS with a throughput of 5000 nm³/h, 10,000 nm³/h, and 30,000 nm³/h, depending on the power of the turbine generator and the gas pressure at the GDS outlet. It is established that when the pressure at the outlet of the P_{out} GDS increases from 0.3 to 1.2 MPa for a generator of a given power, there will be an increase in the required mass flow of gas through the turbine by 2.5 times, the temperature at the outlet of the turbine by 1.12 times, and the outer diameter of the impeller of the vortex turbine by $1.47 \div 1.52$ times depending on the power of the turbogenerator. At the specified gas temperature at the turbine outlet $T_{out} = 273$ K, it is necessary to heat the gas before the turbine generator, which leads to a slight decrease in the diameter of the impeller (by 1–4%) and a significant reduction in gas flow through the turbine generator (by 5–15%) in comparison with the parameters of calculations at a constant gas temperature at the inlet to the turbine $T_{in} = 278$ K. For some turbogenerators, it is possible to perform the design of the turbogenerator in a gearless version with the installation of the impeller of the vortex turbine directly on the shaft of the electric generator. It is proposed to use a vortex turbine, which has advantages over axial and centrifugal turbines, as well as expansion machines of the volumetric principle of operation, which has advantages including the simplicity of design and manufacture, low turnover, reliability of operation, and no mechanical losses in bearings when placing the impeller directly on the generator shaft.

Author Contributions: Conceptualization, S.V., D.S. and D.M.; methodology, S.V., J.P., D.S., D.M., J.M., V.B. and S.M.; software, J.M., V.B. and S.M.; validation, J.P.; formal analysis, J.P.; investigation, S.V., J.P., D.S., D.M., J.M., V.B. and S.M.; resources, D.S., D.M. and V.B.; data curation, S.M.; writing—original draft preparation, D.S., D.M., V.B. and J.M.; writing—review and editing, S.V. and J.M.; visualization, D.S.; supervision, J.M.; project administration, J.P.; and funding acquisition, J.P. All authors have read and agreed to the published version of the manuscript.

Funding: This work was supported by the Slovak Research and Development Agency under contract No. APVV-23-0591, and by the projects VEGA 1/0704/22, KEGA 022TUKE-4/2023 granted by the Ministry of Education, Research, Development and Youth of the Slovak Republic.

Data Availability Statement: The data presented in this study are available on request from the corresponding author.

Acknowledgments: This research was partially supported by the International Association for Technological Development and Innovations and Research and Educational Center for Industrial Engineering (Sumy State University).

Conflicts of Interest: The authors declare no conflicts of interest.

Nomenclature

GDS	gas distribution stations
APR	automatic pressure regulators
RV	regulating valve
C_p	pipe gas velocity
\bar{d}_n	relative nozzle diameter
d_n	diameter of outlet nozzle section
d	diameter of flow path meridional section
\bar{d}_{fp}	relative meridional section diameter of the turbine flow path
D	outer wheel diameter
k	adiabatic index
\bar{u}	circular wheel velocity
η_T	relative internal efficiency of the vortex turbine
η_G	efficiency of the electric generator
P_{in}	inlet pressure
P_{out}	outlet pressure

ρ_{in}	gas density for the turbine inlet
R	gas constant
T_{in}	inlet temperature
N	turbogenerator electric capacity
G	gas mass flow at the vortex expansion machine inlet
Q_T	gas flow at the vortex expansion machine inlet for normal physical conditions

References

- Vaneev, S.; Martsynkovskyy, V.; Hatala, M.; Miroshnichenko, D.; Bilyk, Y.; Smolenko, D.; Lazarenko, A.; Botko, F. Results of the study of a turbogenerator with a peripheral-side channel in non-dimensional and criteria complexes. *MM Sci. J.* **2022**, *2022*, 5913–5917. [CrossRef]
- Kulinchenko, H.; Zhurba, V.; Panych, A.; Leontiev, P. Development of the method of constructing the expander turbine rotation speed regulator. *Eastern-Eur. J. Enterp. Technol.* **2023**, *2*, 44–52. [CrossRef]
- Vaneev, S.; Miroshnichenko, D.; Meleychuk, S.; Baga, V. Research of multi-flow and multi-channel flow parts of the vortex expansion machines with the external peripheral channel. *IOP Conf. Ser. Mater. Sci. Eng.* **2017**, *233*, 012020. [CrossRef]
- Mokhatab, S.; Poe, W.; Mak, J. *Handbook of Natural Gas Transmission and Processing: Principles and Practices*, 4th ed.; Gulf Professional Publishing: Houston, TX, USA, 2019; pp. 121–147. ISBN 978-0-12-815817-3.
- Medvedeva, O.; Polyakov, A.; Kochetkov, A. Technical Solutions to Reduce Natural-Gas Pressure at Gas distribution Stations. *Chem. Pet. Eng.* **2017**, *53*, 469–473. [CrossRef]
- Sa, J.-H.; Zhang, X.; Sum, A. Hydrate management in deadlegs: Effect of driving force on hydrate deposition. *Fuel* **2020**, *279*, 118481. [CrossRef]
- Hu, P.; Chen, D.; Zi, M.; Wu, G. Effects of carbon steel corrosion on the methane hydrate formation and dissociation. *Fuel* **2018**, *230*, 126–133. [CrossRef]
- Wang, J.; Meng, Y.; Han, B.; Liu, Z.; Zhang, L.; Yao, H.; Wu, Z.; Chu, J.; Yang, L.; Zhao, J.; et al. Hydrate blockage in subsea oil/gas flowlines: Prediction, prevention, and remediation. *Chem. Eng. J.* **2023**, *461*, 142020. [CrossRef]
- Klimenko, A.V.; Agababov, V.S.; Koryagin, A.V.; Petin, S.N.; Borisova, P.N. Using an Expander-Generator Unit in the Steel Mill CHP Plant for Producing Electricity and Improving the Efficiency of the Compressor Plant. *Steel Transl.* **2019**, *49*, 587–592. [CrossRef]
- Huang, L. Optimal scheduling of cogeneration microgrid with wind energy and energy storage devices. *IOP Conf. Ser. Earth Environ. Sci.* **2020**, *558*, 052010. [CrossRef]
- Chelabi, M.A.; Saga, M.; Kuric, I.; Basova, Y.; Dobrotvorskiy, S.; Ivanov, V.; Pavlenko, I. The Effect of Blade Angle Deviation on Mixed Inflow Turbine Performances. *Appl. Sci.* **2022**, *12*, 3781. [CrossRef]
- Howard, C.; Oosthuizen, P.; Peppley, B. An investigation of the performance of a hybrid turboexpander-fuel cell system for power recovery at natural gas pressure reduction stations. *Appl. Therm. Eng.* **2011**, *31*, 2165–2170. [CrossRef]
- Englart, S.; Jedlikowski, A.; Capiński, W.; Badura, M. Reducing energy consumption for electrical gas preheating processes. *Therm. Sci. Eng. Prog.* **2020**, *19*, 100600. [CrossRef]
- Danieli, P.; Carraro, G.; Lazzaretto, A. Thermodynamic and Economic Feasibility of Energy Recovery from Pressure Reduction Stations in Natural Gas Distribution Networks. *Energies* **2020**, *13*, 4453. [CrossRef]
- Dabwan, Y.N.; Pei, G.; Kwan, T.H.; Zhao, B. An innovative hybrid solar preheating intercooled gas turbine using parabolic trough collectors. *Renew. Energy* **2021**, *179*, 1009–1026. [CrossRef]
- Xu, X.; Cai, L.; Chen, T.; Zhan, Z. Analysis and optimization of a natural gas multi-stage expansion plant integrated with a gas engine-driven heat pump. *Energy* **2021**, *236*, 121321. [CrossRef]
- Pavlenko, I.; Ciszak, O.; Kondus, V.; Ratushnyi, O.; Ivchenko, O.; Kolisnichenko, E.; Kulikov, O.; Ivanov, V. An Increase in the Energy Efficiency of a New Design of Pumps for Nuclear Power Plants. *Energies* **2023**, *16*, 2929. [CrossRef]
- Pavlenko, I.; Kulikov, O.; Ratushnyi, O.; Ivanov, V.; Pitel', J.; Kondus, V. Effect of Impeller Trimming on the Energy Efficiency of the Counter-Rotating Pumping Stage. *Appl. Sci.* **2023**, *13*, 761. [CrossRef]
- Vanieiev, S.M.; Martsynkovskyy, V.S.; Kulikov, A.; Miroshnichenko, D.V.; Bilyk, Y.I.; Smolenko, D.V.; Lazarenko, A.D. Investigation of a Turbogenerator Based on the Vortex Expansion Machine with a Peripheral Side Channel. *J. Eng. Sci.* **2021**, *8*, F 11–F 18. [CrossRef]
- Vaneev, S.M.; Miroshnichenko, D.V.; Zhurba, V.O.; Znamenshchikov, B.; Baga, V.M.; Rodimchenko, T.S. Stand for the study of low-power expansion vane machines and aggregates based on them. *Refriger. Eng. Technol.* **2019**, *55*, 15–21. [CrossRef]
- Miroshnichenko, D.V. Increasing the Energy Efficiency of Pneumatic Units Created on the Basis of Vortex Expansion Machines: Abstract of the Dissertation. Ph.D. Technical of Science, Spec. 05.05.17–Hydraulic Machines and Hydropneumatic Aggregates, Sumy State University, Sumy. 2019. 23p. Available online: https://essuir.sumdu.edu.ua/bitstream-download/123456789/74957/1/avtoref_Miroshnychenko.pdf (accessed on 20 May 2024).

Disclaimer/Publisher's Note: The statements, opinions and data contained in all publications are solely those of the individual author(s) and contributor(s) and not of MDPI and/or the editor(s). MDPI and/or the editor(s) disclaim responsibility for any injury to people or property resulting from any ideas, methods, instructions or products referred to in the content.